NASA TECHNICAL MEMORANDUM

NASA TM X-2593

NASA TM X-2593

PREDICTED UPWASH ANGLES AT ENGINE INLETS FOR STOL AIRCRAFT

by James A. Albers

Lewis Research Center

Cleveland, Ohio 44135

NATIONAL AERONAUTICS AND SPACE ADMINISTRATION • WASHINGTON, D. C. • JULY 1972

1. Report No.	2. Government Accession No.	3. Recipient's Catalog No.
NASA TM X-2593		

4. Title and Subtitle	5. Report Date
PREDICTED UPWASH ANGLES AT ENGINE INLETS FOR STOL AIRCRAFT	July 1972
	6. Performing Organization Code

7. Author(s)	8. Performing Organization Report No.
James A. Albers	E-6901
	10. Work Unit No.
	741-72

9. Performing Organization Name and Address	11. Contract or Grant No.
Lewis Research Center National Aeronautics and Space Administration Cleveland, Ohio 44135	
	13. Type of Report and Period Covered
12. Sponsoring Agency Name and Address	Technical Memorandum
National Aeronautics and Space Administration Washington, D.C. 20546	14. Sponsoring Agency Code

15. Supplementary Notes

16. Abstract

Upwash angles were predicted for a STOL lifting system by using a two-dimensional potential flow analysis. Upwash angles are presented for distances ahead of the wing leading edge of 50, 75, and 100 percent of wing chord. The upwash angle was determined to be insensitive to the vertical location of the engine inlet. For a wide range of takeoff and landing conditions, the upwash angle was found to be a function of the total two-dimensional lift coefficient. Upwash angles, along with typical flow fields, are presented for a range of total two-dimensional lift coefficients from 2 to 12. Three-dimensional effects were considered in estimating upwash angles for an unswept-wing externally blown flap aircraft. For this STOL configuration, effective upwash angles during takeoff, approach, and waveoff conditions were found to be 22°, 26°, and 36°, respectively.

17. Key Words (Suggested by Author(s))		18. Distribution Statement
Inlet	Potential flow	Unclassified - unlimited
STOL aircraft	Upwash angle	
Flow field	Engines, induction systems	

19. Security Classif. (of this report)	20. Security Classif. (of this page)	21. No. of Pages	22. Price*
Unclassified	Unclassified	16	$3.00

* For sale by the National Technical Information Service, Springfield, Virginia 22151

PREDICTED UPWASH ANGLES AT ENGINE INLETS FOR STOL AIRCRAFT

by James A. Albers

Lewis Research Center

SUMMARY

Upwash angles were predicted for a STOL lifting system by using a two-dimensional potential flow analysis. Upwash angles are presented for distances ahead of the wing leading edge of 50, 75, and 100 percent of wing chord. The upwash angle was determined to be insensitive to the vertical location of the engine inlet. For a wide range of takeoff and landing conditions, the upwash angle was found to be a function of the total two-dimensional lift coefficient. Upwash angles, along with typical flow fields, are presented for a range of total two-dimensional lift coefficients from 2 to 12. Three-dimensional effects were considered in estimating upwash angles for an unswept-wing externally blown flap aircraft. For this STOL configuration, effective upwash angles during takeoff, approach, and waveoff conditions were found to be 22°, 26°, and 36°, respectively.

INTRODUCTION

One of the requirements that must be considered in designing engine inlets for STOL airplanes is the upwash angle at the inlet during low-speed operation. Because of the high lift coefficients necessary for takeoff and landing operation of STOL aircraft, the engine inlet will be exposed to larger upwash angles than inlets for conventional aircraft. This complicates the inlet design of the nacelles, which must be designed to supply high-pressure recovery and uniform flow to the engine compressor during low-speed and cruise operation (ref. 1). During low-speed operation, the large upwash angles cause low static pressures to develop on the lower inlet lip of the nacelle (ref. 2). These low static pressures produce adverse pressure gradients that can cause flow separation. By knowing the upwash angle design requirement at the engine inlet during takeoff and approach conditions, the designer is better equipped to design the internal lip and diffuser geometry to avoid flow separation, thereby minimizing inlet pressure losses and flow distortions.

Upwash angles can be determined from two-dimensional potential flow analysis of STOL wing propulsion systems (ref. 3). Flow fields of wing propulsion systems with the engine inlet located at or aft of the wing leading edge are briefly discussed in reference 4. The present study utilizes the analysis of reference 3 to predict upwash angles at points in the flow field ahead of the wing leading edge. These upwash angle locations are applicable for STOL concepts presently being developed, such as the externally blown flap configuration (ref. 5) and the augmentor wing configuration.

The objective of this report is to present upwash angles that may be encountered at the engine inlet during takeoff and approach conditions. This study was made for a range of lift coefficients from 2 to 12. Upwash angles, along with typical flow fields, are presented for distances ahead of the wing leading edge of 50, 75, and 100 percent of chord. The sensitivity of the upwash angle to the vertical position of the inlet is illustrated. Three-dimensional effects were considered in estimating upwash angles for an externally blown flap aircraft during takeoff, approach, and waveoff conditions.

SYMBOLS

b	wing span
C_L	three-dimensional lift coefficient, L/qS
C_l	total two-dimensional lift coefficient, L/qc
C_μ	jet momentum coefficient at flap trailing edge, $m_j V_j/qc$
c	chord length (fig. 1)
h	perpendicular distance from vortex core to point p (fig. 4)
L	total lift of wing, flap, and jet
m	mass flow rate
p	point at engine inlet location (fig. 4)
q	free-stream dynamic pressure
S	wing planform area
V	velocity
X	distance perpendicular to vortex filament (fig. 4)
x	axis parallel to wing chord line (fig. 1)
x'	axis parallel to free-stream velocity (fig. 1)
y	axis perpendicular to wing chord line (fig. 1)

y' axis perpendicular to free-stream velocity (fig. 1)

z distance along wing span (fig. 1)

α, β angles defined in fig. 4

α_e angle of attack of engine; angle between free-stream velocity and engine axis (fig. 1)

α_i engine incidence angle; angle between engine axis and wing chord line (fig. 1)

α_w angle of attack of wing; angle between free-stream velocity and wing chord line (fig. 1)

Γ vortex strength per unit length

δ jet angle at flap trailing edge; angle between free-stream direction and lower flap surface (fig. 1)

θ upwash angle at inlet lower lip; angle between free-stream velocity vector and resultant local velocity vector (fig. 1)

θ_e effective upwash angle at inlet lower lip; angle between engine axis and resultant local velocity vector (fig. 1)

Subscripts:

av average

en engine location

id induced by vortex filament

j jet

max maximum

p lower inlet lip location

R resultant at inlet lip

∞ free stream

METHOD OF ANALYSIS

Two-Dimensional Upwash Angle

The notation and coordinate system used in this report are shown in figure 1. The upwash angle θ is defined as the angle between the free-stream velocity vector and the resultant local velocity vector at the lower inlet lip. The effective upwash angle at the

lower lip θ_e is defined as the angle between the engine axis and the resultant local velocity vector at the lower inlet lip. Thus

$$\theta_e = \theta + \alpha_e \tag{1}$$

where α_e is the angle of attack of the engine. The angle of attack of the engine was determined from the angle of attack of the wing and the engine incidence relative to the wing chord. Thus

$$\alpha_e = \alpha_w + \alpha_i \tag{2}$$

Upwash angles were calculated by considering the two-dimensional lifting system shown in figure 2. The lifting system is represented by a combined airfoil and flap and a jet sheet leaving the flap trailing edge. The effect of the inlet airflow of the engine was not considered in this analysis. The jet momentum coefficient at the flap trailing edge C_μ is based on the jet momentum at the engine exit. The potential flow solution for the lifting system was determined by the method of reference 3. This method utilizes a distribution of sources and sinks on the airfoil and flap surface and approximates the location of the exhaust jet of the propulsion system. Upwash angles were determined by calculating local velocity vectors at various positions in the flow field. The coordinate axes x', y' for the flow field are taken to be parallel and perpendicular to the free-stream velocity (fig. 1). The upwash angle is expressed as

$$\theta = \arctan \frac{V_{y'}}{V_{x'}} \tag{3}$$

and the resultant local velocity is expressed as

$$V_R = \sqrt{(V_{x'})^2 + (V_{y'})^2} \tag{4}$$

Three-Dimensional Effects on Upwash Angle

Three-dimensional effects must be considered in estimating the upwash angles for an actual STOL configuration. This section describes a method of calculating upwash angles for a three-dimensional lifting system by accounting for the spanwise loading distribution. A representative externally blown flap STOL configuration has a nonuni-

form spanwise loading distribution, with maximum loading occurring at the engine locations as shown in figure 3. This figure, obtained from unpublished data, illustrates the nondimensional loading $cC_l/c_{en}C_{l,max}$ as a function of percent semispan $z/(b/2)$. The solid curve represents a highly loaded wing at the engine locations with an average total lift coefficient of about 8.0. The dashed curve represents a moderately loaded wing at the engine locations, with an average total lift coefficient of about 4.0. The spanwise loading falls off rapidly with distance from an engine location.

The effect of the nonuniform spanwise loading distribution on the upwash angle can be estimated by calculating the induced velocity at the engine inlet location from the spanwise circulation distribution $\Gamma(\gamma)$ corresponding to the loading distribution. The effect of the nonuniform spanwise loading distribution was obtained by replacing the wing by a lifting vortex filament of strength $\Gamma(\gamma)$ located at the wing center of pressure. The Biot-Savart law was then used to determine the velocity induced by the vortex filament (fig. 4). Then, the induced velocity at point p became

$$V_{id,p} = \int_{\gamma=\alpha}^{\gamma=\pi-\beta} \frac{\Gamma(\gamma)}{4\pi h} \sin\gamma \, d\gamma \tag{5}$$

The strength of the vortex filament $\Gamma(\gamma)$ is directly proportional to the nondimensional spanwise loading distribution $cC_l/c_{en}C_{l,max}$. Comparing the velocity induced at point p from a distribution of vortex strength (three dimensional) to that of a constant vortex strength (two dimensional) gave the percent reduction of the three-dimensional induced velocity from the two-dimensional value. As an example, the loading distribution of the dashed curve of figure 3 resulted in a 29 percent reduction, from the two-dimensional value, in the induced velocity at point p. The corresponding reduction in upwash angle was then computed by using equation (3).

DISCUSSION

Two-Dimensional Upwash Angle and Resultant Local Velocity for Various Longitudinal Positions of Inlet

The two-dimensional upwash angle θ for various inlet positions is shown in figure 5 for total two-dimensional lift coefficients ranging from 2 to 12. The wide range of total two-dimensional lift coefficients was obtained by varying the wing angle of attack, the jet angle at the flap trailing edge, and the jet momentum coefficient. The range of these parameters was as follows: wing angle of attack, zero to 20°; jet angle, 30° to 60°;

and jet momentum coefficient, 1 to 4. Representative values of these parameters at various lift coefficients are shown in figure 5(a). The jet momentum coefficients shown were calculated for a free-stream Mach number of 0.12. The upwash angle for a specified inlet location was found to be a function only of the total two-dimensional lift coefficient regardless of the combination of angle of attack, jet angle, and jet momentum coefficient used to obtain the lift coefficient. As the inlet position was moved further ahead of the wing leading edge (from x/c of -0.5 to -1.0) for the same vertical position ($y/c = -0.4$), there was approximately a 35 percent reduction in the upwash angle. For a typical inlet location of $x/c = -0.75$, the upwash angle varied from 8.5° at a C_l of 2 to 37° at a C_l of 12.

The resultant velocity V_R at the inlet lip (fig. 1) corresponding to these upwash angles must also be considered when designing inlets for STOL engines (fig. 5(b)). The resultant local velocity varied from 0.89 of the free-stream velocity at a lift coefficient of 2 to 1.24 of the free-stream velocity at a lift coefficient of 12 for longitudinal positions ranging from x/c of -0.5 to -1.0 ($y/c = -0.4$). The resultant local velocity varied on the average of 3 percent as x/c ranged from -0.5 to -1.0 at a constant value of lift coefficient.

Two-Dimensional Upwash Angle and Resultant Local Velocity for Various Vertical Positions of Inlet

The sensitivity of upwash angle at the engine inlet to the vertical position of the engine is illustrated in figure 6(a) at three longitudinal engine inlet locations at a total two-dimensional lift coefficient of 4.7. The upwash angle was insensitive to vertical location of the lower inlet lip for values of y/c ranging from -0.2 to -0.5. This result was found to be true over the entire range of lift coefficients considered (2 to 12).

The resultant local velocity was also insensitive to the vertical position of the lower inlet lip for values of y/c ranging from -0.2 to -0.5 (fig. 6(b)). This result was found to be true for longitudinal locations x/c ranging from -0.5 to -1.0 and lift coefficients ranging from 2 to 12.

Two-Dimensional Effective Upwash Angles for Various Angles of Attack of Engine

The effective upwash angle was obtained from equation (1) by adding the engine angle of attack to the calculated upwash angles of figure 5(a). Effective upwash angles for a typical lower inlet lip location of $x/c = -0.75$ and $y/c = -0.4$ are shown in figure 7 for angles of attack of the engine ranging from 0° to 16°. Effective upwash angles varied

from 9° (corresponding to α_e of 0° and C_l of 2.0) to 49° (corresponding to α_e of 16° and C_l of 12.0). The effective upwash angle defines the angle-of-attack requirement for isolated nacelle testing and the angle-of-attack tolerance for the inlet designer. Representative effective upwash angles for a STOL externally blown flap configuration are discussed in the following section.

Application to Externally Blown Flap Configuration

To illustrate the application of the predicted upwash angle to a STOL aircraft configuration, an externally blown flap (EBF) aircraft with an unswept wing was considered. Representative three-dimensional lift coefficients and angles of attack for this configuration during takeoff, approach, and constant-speed waveoff (constant lift coefficient but reduced flap setting) conditions are shown in table I. The angle of attack of the engine α_e was obtained by use of equation (2), assuming $\alpha_i = -3^{\circ}$.

If the preceding values of three-dimensional lift coefficient were taken to be the total section lift coefficient at the inlet location, the effective upwash angles as determined from figure 7 were 20.5° for takeoff, 23.5° for approach, and 33.5° for waveoff. However, these values of upwash angle do not include any effects of the nonuniform spanwise loading distribution of the wing. The method used to account for the loading distribution was presented in the section METHOD OF ANALYSIS. For this example, the loading distribution of the dashed curve of figure 3 was used. This loading distribution is representative for a four-engine externally blown flap aircraft. First, the total section lift coefficient at the engine location was determined by dividing the three-dimensional lift coefficient by the average value of the loading distribution nondimensionalized with respect to the cC_l at the engine location. For this example, at the inboard engine location the lift coefficient and corresponding effective upwash angle as determined from figure 7 (assuming an inlet position of $x/c = -0.75$ and $y/c = -0.4$) for takeoff, approach, and waveoff conditions are shown in table II. The method of the analysis section was then used to calculate the values of upwash angle accounting for the spanwise loading distribution. This calculation resulted in a 15 to 20 percent reduction of effective upwash angle from the two-dimensional value. The values of effective upwash angle accounting for the loading distribution are given in table III. The results of the analysis indicate that the two-dimensional values of the effective upwash angle are about 10 percent higher than the effective upwash angle corresponding to the three-dimensional lift coefficient.

The preceding values indicate that the upwash angle for a STOL configuration is quite large and is probably a major factor in effecting the design of the engine inlet lip and diffuser.

The upwash angle at the engine inlet for a given STOL aircraft could be reduced if the total two-dimensional lift coefficient at the engine location could be reduced while maintaining the same wing lift coefficient. This could be accomplished by having a more uniform spanwise variation of lift coefficient. The lift coefficient can be made more uniform by effectively spreading the engine exhaust across the span of the wing.

Flow Fields

Typical flow fields of a two-dimensional STOL lifting system are shown in figure 8. A representative engine location with inlet at $x/c = -0.75$ and $y/c = -0.4$ is illustrated with dotted lines. The flow fields were obtained by sketching streamlines tangent to the calculated velocity vectors at various points in the flow. The upwash ahead of the wing leading edge is proportional to the downwash aft of the wing trailing edge. At the low lift coefficient (fig. 8(a)), the jet leaving the flap trailing edge penetrates a relatively small distance in the flow, resulting in small upwash angles at the engine inlet of the order of 15°. At the higher lift coefficients corresponding to higher angles of attack and jet angle (figs. 8(b) and (c)), the jet leaving the flap trailing edge penetrates more into the free stream. Jet penetration increases as jet angle and jet momentum coefficient are increased. These large jet penetrations result in large upwash angles at the engine inlet at the higher lift coefficients.

SUMMARY OF RESULTS

Upwash angles were predicted for engine inlets at locations ahead of the wing leading edge. They were predicted from velocity fields of a two-dimensional potential flow analysis of a STOL lifting system. For this study, the wing angle of attack ranged from 0° to 20°; the jet incidence angle ranged from 30° to 60°; and the jet momentum coefficient ranged from 1 to 4. The principal results of this study are as follows:

1. The upwash angle was a function of the total two-dimensional lift coefficient regardless of the combination of wing angle of attack, jet incidence angle, and jet momentum coefficient considered.

2. For a typical inlet lip location ($x/c = -0.75$, $y/c = -0.4$) the upwash angle varied from 8° at a lift coefficient of 2 to 37° at a lift coefficient of 12. The resultant local velocity varied from 0.89 of the free-stream velocity at a lift coefficient of 2 to 1.24 of the free-stream velocity at a lift coefficient of 12 at the same inlet location.

3. The upwash angle decreased as the inlet lip longitudinal location was moved further ahead of the wing leading edge. The resultant local velocity varied on the average of 3 percent as x/c ranged from -0.5 to -1.0 at a constant value of lift coefficient.

4. The upwash angle and resultant local velocity were insensitive to the vertical location of the inlet lip.

5. Three-dimensional effects were considered in estimating the upwash angles for an externally blown flap configuration. The effective upwash angles during takeoff, approach, and waveoff conditions were found to be 22°, 26°, and 36°, respectively.

6. Flow fields of a jet flap lifting system indicated large penetration of the jet exhaust leaving the flap trailing edge during takeoff and landing conditions. This resulted in large upwash angles at locations in the flow ahead of the wing leading edge.

Lewis Research Center,
National Aeronautics and Space Administration,
Cleveland, Ohio, May 2, 1972,
741-72.

REFERENCES

1. Douglass, W. M.: Aerodynamic Installation of High-Bypass-Ratio Fan Engines. Paper 660732, SAE, Oct. 1966.

2. Hancock, J. P.; and Hinson, B. L.: Inlet Development for the L-500. Paper 69-448, AIAA, June 1969.

3. Albers, James A.; and Potter, Merle C.: Potential Flow Solution for a STOL Wing Propulsion System. NASA TN D-6394, 1971.

4. Albers, James A.: Analysis of the Effect of Engine Characteristics on the External Aerodynamics of STOL Wing Propulsion Systems. NASA TM X-2541, 1972.

5. Parlett, Lysle P.; Greer, H. Douglas; Henderson, Robert L.; and Carter, C. Robert: Wind-Tunnel Investigation of an External-Flow Jet-Flap Transport Configuration Having Full-Span Triple-Slotted Flaps. NASA TN D-6391, 1971.

TABLE I. - THREE-DIMENSIONAL LIFT COEFFICIENTS AND ANGLES OF ATTACK FOR EBF STOL AIRCRAFT

Condition	Three-dimensional lift coefficient, C_L	Angle of attack of wing, α_w, deg	Angle of attack of engine, α_e, deg
Takeoff	3.2	11	8
Approach	4.7	9	6
Waveoff	4.7	19	16

TABLE II. - TWO-DIMENSIONAL LIFT COEFFICIENTS AND UPWASH ANGLES FOR EBF STOL AIRCRAFT

Condition	Total two-dimensional lift coefficient, C_l	Effective upwash angle, θ_e, deg
Takeoff	5.1	27.0
Approach	7.5	32.5
Waveoff	7.5	42.5

TABLE III. - UPWASH ANGLES FOR EBF STOL AIRCRAFT ACCOUNTING FOR SPANWISE LOADING DISTRIBUTION

Condition	Effective upwash angle, θ_e, deg
Takeoff	22
Approach	26
Waveoff	36

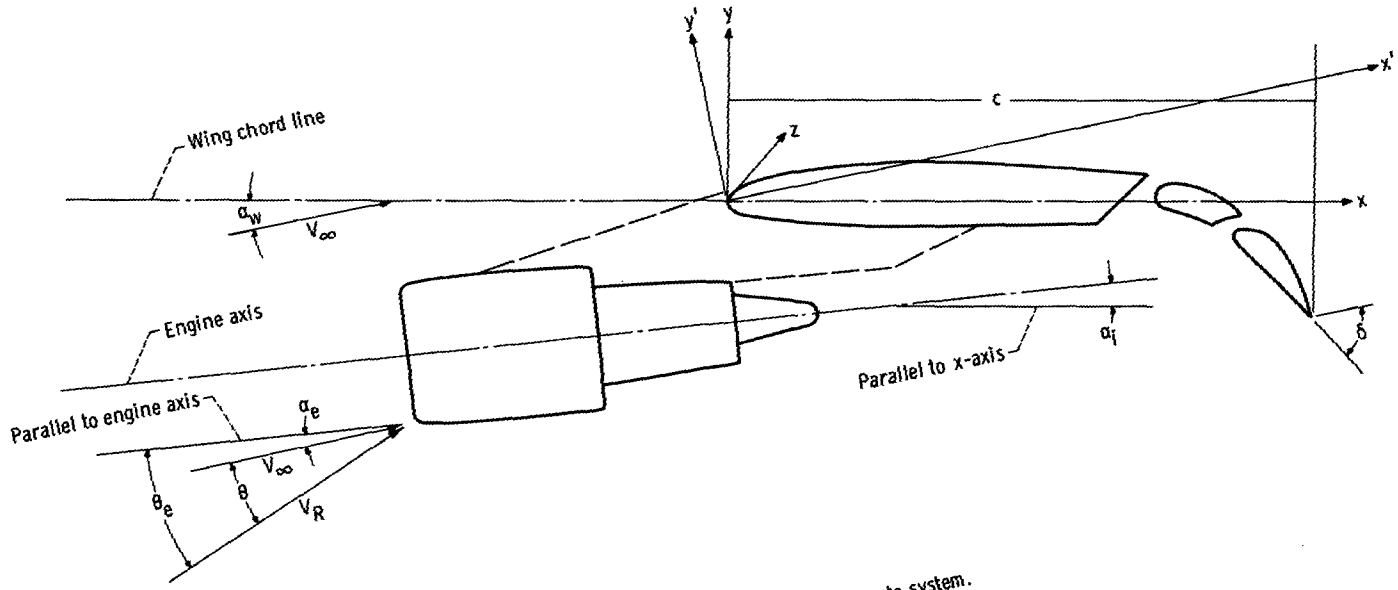

Figure 1. - Notation and coordinate system.

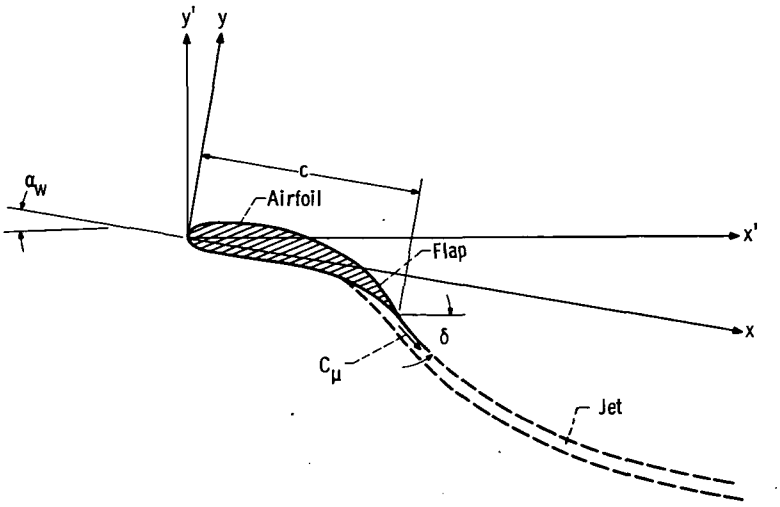

Figure 2. - Representation of two-dimensional jet flap lifting system.

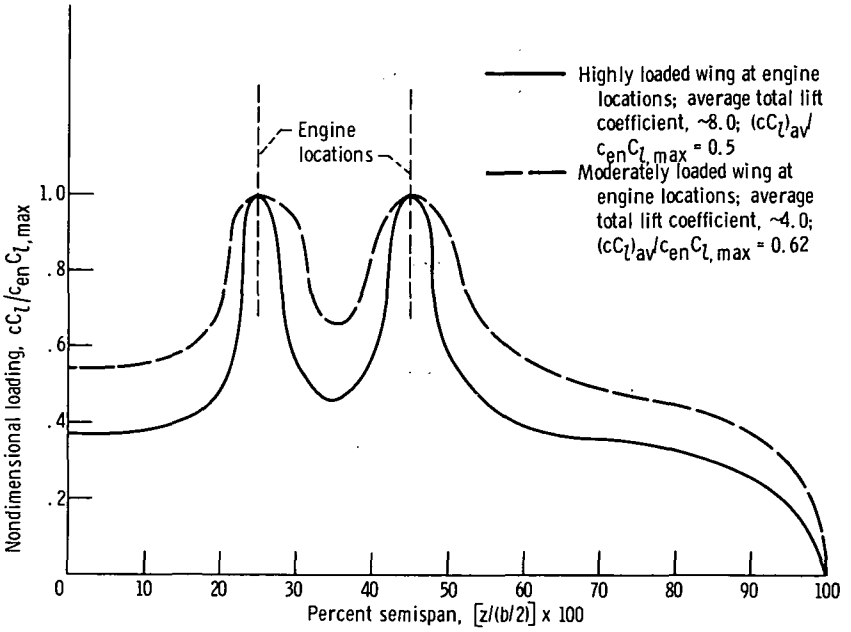

Figure 3. - Spanwise loading distributions for externally blown flap aircraft.

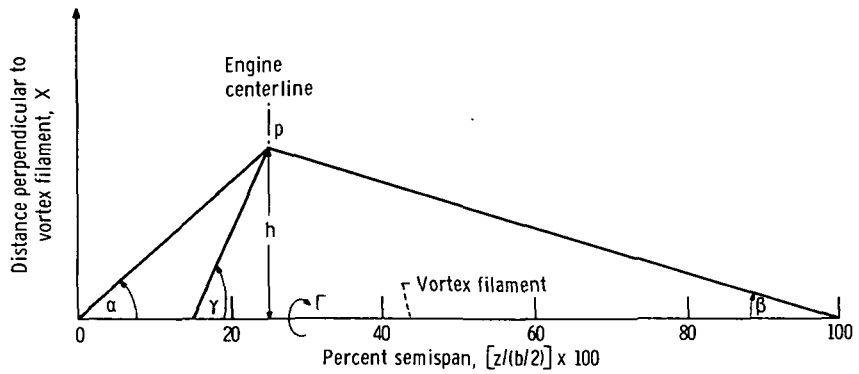

Figure 4. - Notation for Biot-Savart law.

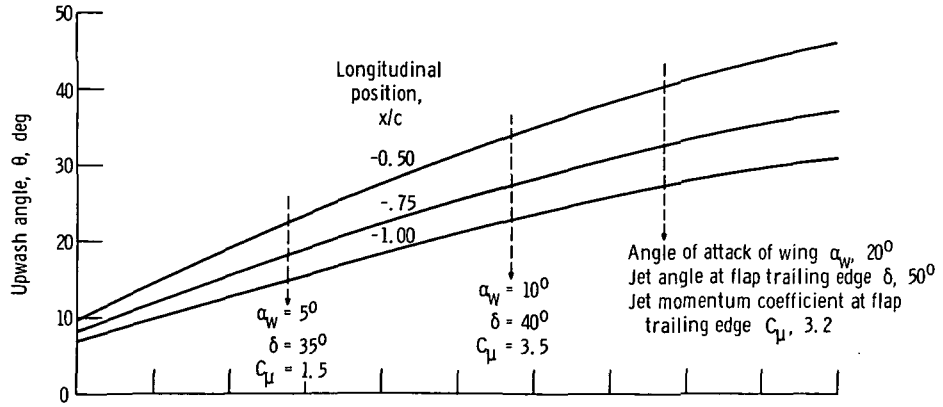

(a) Upwash angle.

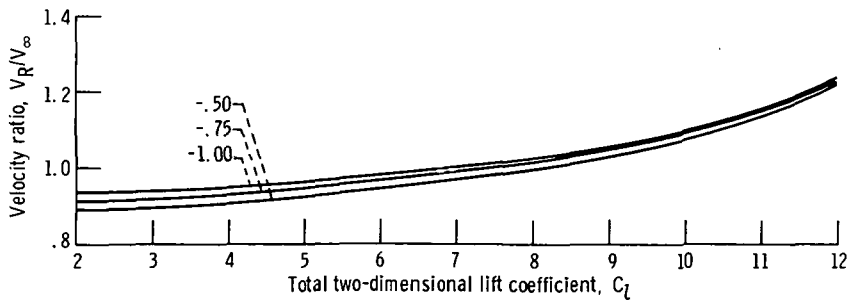

(b) Resultant local velocity.

Figure 5. - Upwash angle and resultant local velocity for various longitudinal positions of inlet. Vertical position y/c, -0.4.

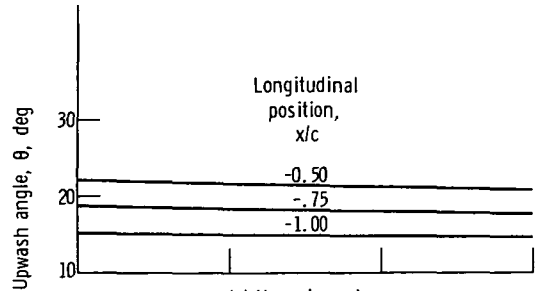

(a) Upwash angle.

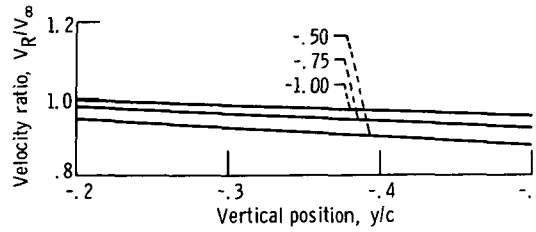

(b) Resultant local velocity.

Figure 6. - Upwash angle and resultant local velocity for various vertical positions of inlet. Total two-dimensional lift coefficient C_l, 4.7.

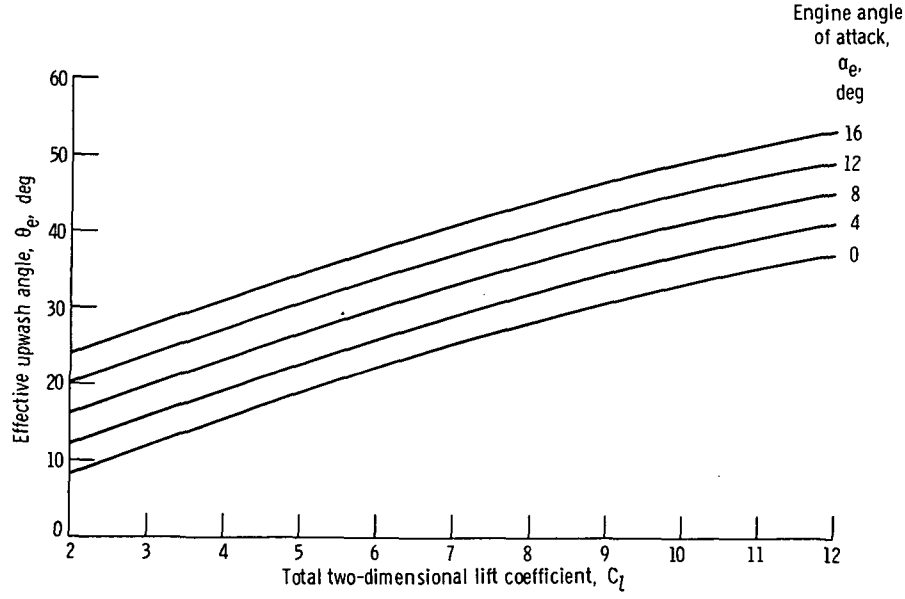

Figure 7. - Effective upwash angle for various angles of attack of engine. Engine location: longitudinal position x/c, -0.75; vertical position y/c, -0.4.

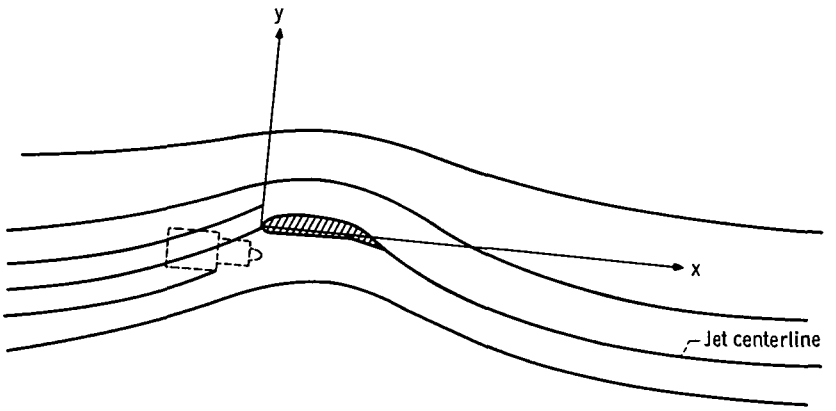

(a) Total two-dimensional lift coefficient, 4.75; wing angle of attack, 5^{0}; jet angle, 35^{0}; jet momentum coefficient, 3.2.

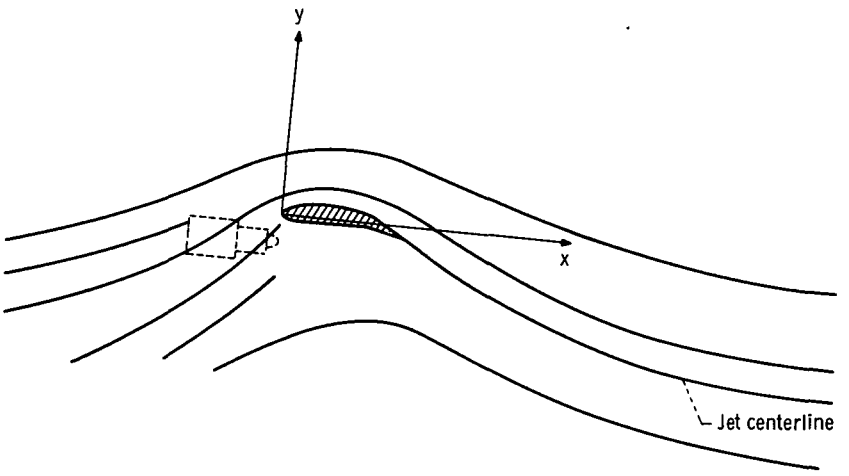

(b) Total two-dimensional lift coefficient, 8.2; wing angle of attack, 10^{0}; jet angle, 40^{0}; momentum coefficient, 3.4.

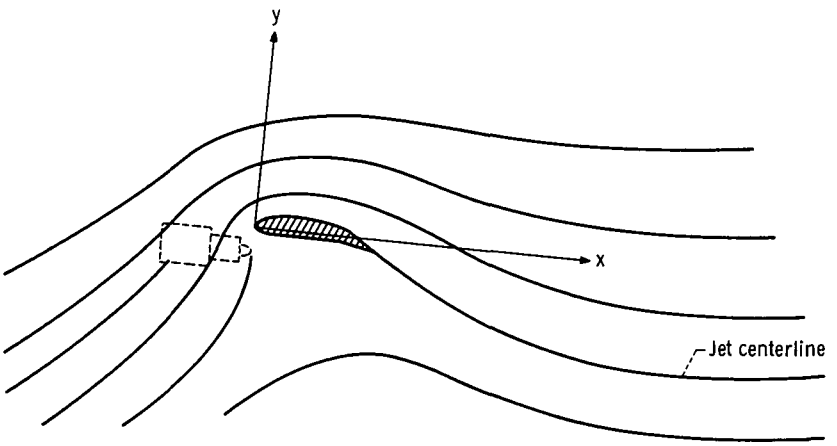

(c) Total two-dimensional lift coefficient, 9.75; wing angle of attack, 20^{0}; jet angle, 50^{0}; jet momentum coefficient, 1.5.

Figure 8. - Flow fields at various lift coefficients. Engine location: longitudinal position x/c, -0.75; vertical position y/c, -0.4.

"The aeronautical and space activities of the United States shall be conducted so as to contribute . . . to the expansion of human knowledge of phenomena in the atmosphere and space. The Administration shall provide for the widest practicable and appropriate dissemination of information concerning its activities and the results thereof."

—NATIONAL AERONAUTICS AND SPACE ACT OF 1958

NASA SCIENTIFIC AND TECHNICAL PUBLICATIONS

TECHNICAL REPORTS: Scientific and technical information considered important, complete, and a lasting contribution to existing knowledge.

TECHNICAL NOTES: Information less broad in scope but nevertheless of importance as a contribution to existing knowledge.

TECHNICAL MEMORANDUMS: Information receiving limited distribution because of preliminary data, security classification, or other reasons.

CONTRACTOR REPORTS: Scientific and technical information generated under a NASA contract or grant and considered an important contribution to existing knowledge.

TECHNICAL TRANSLATIONS: Information published in a foreign language considered to merit NASA distribution in English.

SPECIAL PUBLICATIONS: Information derived from or of value to NASA activities. Publications include conference proceedings, monographs, data compilations, handbooks, sourcebooks, and special bibliographies.

TECHNOLOGY UTILIZATION PUBLICATIONS: Information on technology used by NASA that may be of particular interest in commercial and other non-aerospace applications. Publications include Tech Briefs, Technology Utilization Reports and Technology Surveys.

Details on the availability of these publications may be obtained from:

SCIENTIFIC AND TECHNICAL INFORMATION OFFICE

NATIONAL AERONAUTICS AND SPACE ADMINISTRATION

Washington, D.C. 20546